Available online at www.derpharmachemica.com

ISSN 0975-413X
CODEN (USA): PCHHAX

Der Pharma Chemica, 2016, 8(19):350-358
(http://derpharmachemica.com/archive.html)

Spectroscopic evidence for binding of benzylidene piperidone with bovine serum albumin

Madhavi Changa[a], Nithya Pattusamy[b*] and Krishnendu Biswas[a*]

[a]*Chemistry Division, School of advanced sciences, VIT University, Chennai-600127, Tamilnadu, India*
[b]*Department of chemistry, Bharathi women's college, Chennai-600108, Tamilnadu, India*

ABSTRACT

The interaction between benzylidene piperidone (BzP) and bovine serum albumin (BSA) was investigated by spectroscopic techniques. It was observed that BzP has a strong ability to quench the intrinsic fluorescence of BSA through static quenching. The binding constant 'K' and number of binding sites 'n' were calculated, and Gibbs free energy [ΔG^0] change was found to be negative. The negative ΔG^0 values confirmed that the binding process is spontaneous. The conformation changes of BSA investigated by synchronous, and circular dichroism spectra revealed the changes in the secondary structure of BSA upon interaction with BzP. Synchronous fluorescence spectra showed a change from red to blue shift which is an indication of increasing hydrophobicity.

Keywords: Benzylidene piperidone, Bovine serum albumin, Circular dichroism, Fluorescence studies, Synchronous fluorescence, Quenching.

INTRODUCTION

It is known that the drug-protein interactions in the blood stream affects the distribution, free concentration and the metabolism of various drugs [1]. Interactions between drug and protein are important, as most of the drugs that are administered are widely and reversibly bound to the protein serum albumin. They are carried mainly to the target cells as a complex with proteins. The nature and extent of drug-protein binding interactions extensively influence the biological activity of the drug [2-3]. Accordingly, the analysis of the binding between the drugs and serum albumin is of fundamental importance of pharmacological studies and the parameters of binding are helpful in studying the action of drugs [4-5]. The studies of the binding of drugs to BSA provide information of structural characteristics that determine the therapeutic efficiency of drugs and become an significant research field in chemistry and clinical medicine [6].

Bovine serum albumin (BSA) was selected as a protein model because its widely used in molecular biological experiments due to its low cost and ready availability. However, BSA is the most abundant carrier protein for unesterified fatty acids present in plasma, also capable of binding an extremely various range of drugs, dyes and organic compounds [7]. Since the efficiency of many drugs in the body are correlated with their extent of binding with serum albumin, their interaction studies are vital [8-11]

Benzylidene piperidone (BzP) is one such compound having cytotoxic, anticancer, antioxidant, anti-inflammatory, analgesic, antiviral, antipyretic activities [12]. The heterocyclic analogs of chalcones show very strong interaction with the BSA making changes to its secondary structure [13]. Owing to the fewer reports in the literature on the interaction studies of BSA with BzP, we have carried out the binding studies of BSA with BzP using various spectroscopic techniques in the present work.

MATERIALS AND METHODS

2.1. Reagents and chemicals

Bovine serum albumin (BSA) procured from Sigma Aldrich, benzaldehyde, ethylmethylketone, methanol, NaOH was purchased from SD fine chemicals, India. BzP and BSA solutions were prepared in 0.1 M phosphate buffer with pH 7.4 containing 0.15 M NaCl. All other chemicals were of analytical reagent grade and used without any further purification.

2.2. Spectral measurements

Fluorescence spectra were recorded using a Model F-7000 FL Spectrophotometer Hitachi Serial Number, 2573-001 with a 150 W Xenon lamp, 1 cm quartz cell, and a thermostatic cuvette holder. The excitation and emission bandwidths were both 5 nm. The BSA solution was prepared using phosphate buffer with millipore water and maintained at 4 ^{0}C. The absorption spectra were recorded using a double beam U-2900 Spectrophotometer in the range of 200-400 nm and FT-IR Thermo scientific-Nicolet iS10 was use to record infrared spectra in the range of 4000-400 cm^{-1}. Circular dichroism (CD) was recorded in JASCO Corp., J-715 model in the range of 200 – 250 nm. pH measurements were carried out using Elico LI120 pH meter (Elico Ltd., India).

2.3. Synthesis of benzylidene piperidone (BzP)

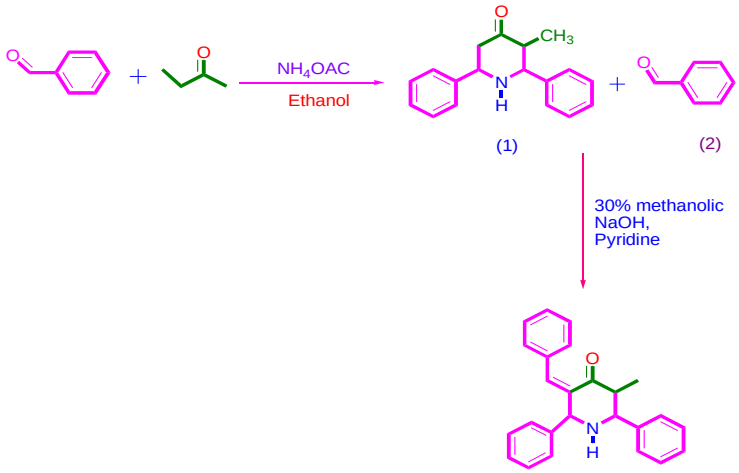

Fig. 1. Scheme depicting the synthesis of (Z) - 3-benzylidene-5-methyl-2, 6-diphenyl piperidin-4-one

(Z) - 3-benzylidene-5-methyl-2, 6-diphenyl piperidin-4-one was synthesized following literature report following the scheme given in Fig. 1 [14-15]. A mixture of 3-methyl-2, 6-diphenylpiperidin-4-one (0.01 mol) and aromatic aldehyde (0.01 mol) was taken in a 100 ml round bottom flask containing 10 ml of ethanol, heated under reflux for 30 min and pyridine (1ml) was added to the reaction mixture. After 5h, formation of a solid product was observed. The reaction mixture was cooled to room temperature and the solid product was filtered and washed with a cold mixture of ethanol and water. The crude product was purified by recrystallization from 95% ethanol to get the pure product and the yield of the product was found to be 85%.

2.4. BzP–Protein interaction study

On the source of initial experiments, 10 samples were made keeping BSA concentration fixed at 12 μM and drug concentration being varied from 20 to 200 μM with an interval of 20 μM. Fluorescence spectra for each sample were recorded at different temperatures 288, 298, 308, 318, 328 K, in the wavelength range of 300–500 nm upon excitation at 286 nm. UV measurements were also carried on the same samples using phosphate buffer at room temperature. The CD spectra of BSA which is dissolved in phosphate buffer with and without BzP were recorded using 20 μM and 40 μM concentration of BzP. The FT-IR spectra of the BSA with and without of BzP were recorded to confirm their interactions. Synchronous fluorescence spectra were recorded with scan ranges, $\Delta\lambda$=15 nm and 60 nm ($\Delta\lambda=\lambda_{em}-\lambda_{ex}$) in the absence and presence of BzP and the spectra were recorded in the range of 250–400 nm. 3D fluorescence spectra were recorded with excitation wavelength range of 200-800 nm and concentration of BzP of 12, 20, 40 and 60 μM.

RESULT AND DISCUSSION

3.1. Fluorescence quenching studies of BSA by BzP

The fluorescence spectra of all the samples recorded in the range of 300-500 nm upon excitation at 286 nm is shown in Fig. 2. It is clear from the fluoresnce spectra that varying concentration of BzP causes a quenching of the intrinsic

fluorescence of BSA without any change in emission maximum. These results indicated that there is an interactions between BzP and BSA. The fluorescence quenching data were analyzed by the Stern-Volmer equation.

$$\frac{F_0}{F} = 1 + K_{SV}[Q] = 1 + K_q\tau_0[Q] \quad (1)$$

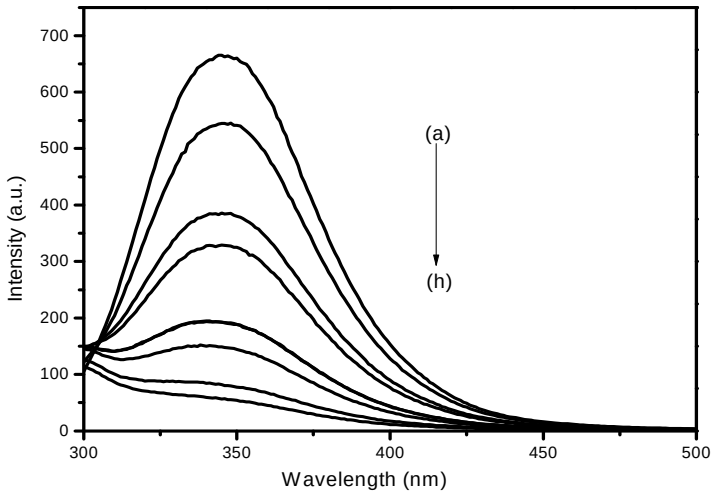

Fig. 2. Fluorescence spectra of BSA (a) 12 µM in the presence of BzP: (b) 20 µM, (c) 40 µM, (d) 60 µM, (e) 80 µM, (f) 100 µM, (g) 120 µM, (h) 140 µM (a-h)

Where F and F_0 are the fluorescence intensity of BSA with and without quencher (BzP). Kq is the quenching rate constant of the bio molecule, k_{sv} is the Stern-Volmer quenching constant, τ_0 is the average lifetime of bio molecule without the quencher and [Q] is the concentration of the quencher. The Stern-Volmer plots shown in Fig. 3 are found to be linear with slope (K_{sv}) value decreasing with increasing concentration of BzP.

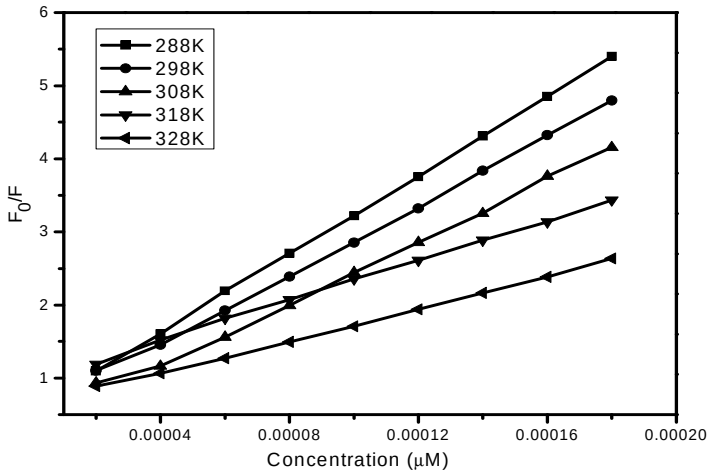

Fig. 3. The Stern-Volmer curves showing quenching of BSA, [BSA] = 12 µM

The Stern-Volmer plot did not show difference towards the y-axis at the various concentration ranges, which shows the signal of either dynamic or static quenching was predominant. The grades of interaction carried out at diverse temperatures (288, 298, 308, 318, 328 K) were found to be linear with slopes (K_{SV} values) decreasing with increasing temperatures (Fig. 3). The values of K_{SV} for BzP-BSA system at different temperatures were calculated to be 4.0749 x 10^4, 2.6873 x 10^4, 2.0771 x 10^4, 1.3758 x 10^4, 1.0976 x 10^4 L mol^{-1} respectively indicating static quenching interface between BzP-BSA. Further, the rate constant for the bio molecular quenching process, Kq were evaluated using the Eq. (2)

$$K_q = \frac{K_{SV}}{\tau_0} \quad (2)$$

Since the fluorescence lifetime τ_0 of the bio molecule was 10^{-8} s [16], the value Kq for BzP–BSA system was calculated as 4.0749 x 10^{12}, 2.6873 x 10^{12}, 2.0771 x 10^{12}, 1.3758 x 10^{12}, 1.0976 x 10^{12} L mol^{-1} s^{-1} at 288, 298, 308, 318, 328 K respectively. Since the values of Kq obtained are higher than Kq of scatter procedure, which is 2 x 10^{10} L mol^{-1} S^{-1}. It is clear that the quenching was not initiated by dynamic collision but from the development of a complex. This indicates that a static quenching mechanism is effective.

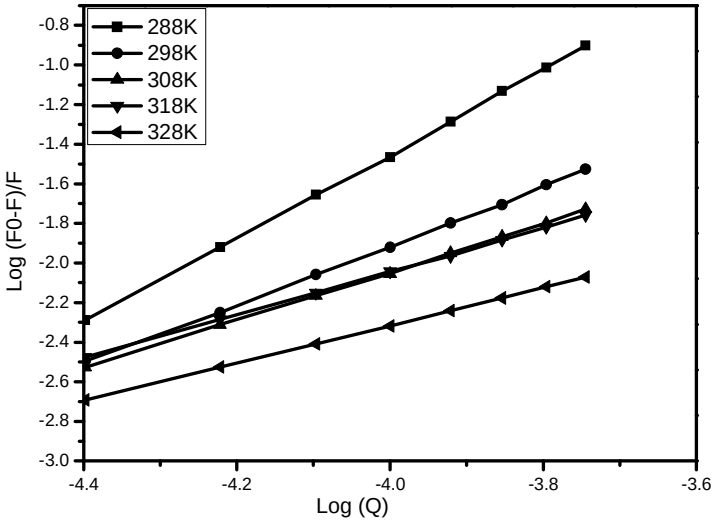

Fig. 4. The Stern-Volmer curves showing quenching of BSA, [BzP] = 20-140 µM, [BSA] = 12 µM

BSA-BzP interaction was further confirmed by varying the concentrations of BzP. From the results, it can be inferred that there is an existence of good linearity at lower concentrations (20-140 µM) as well as a single quenching mechanism shown by BzP in the binding process. Hence, it is confirmed that the interaction between BSA-BzP is a static quenching.

3.2. Binding constant and the number of binding sites

When small molecules unite independently to a set of equivalent sites on a macromolecule, fluorescence intensity data can be used to acquire the binding constant K and the number of binding sites n. by the following Eq. (3).

$$\log \frac{F_0 - F}{F} = \log K_a + n \log[Q] \quad (3)$$

The values of K and n were calculated from the intercept and slope of the straight line obtained from the plot of log $[(F_0 - F) / F]$ versus log [Q] given in Fig. 4. It is clear from the values of K and n given in table 1 that the binding constant increased with raise in temperature suggesting that the interactions involved in the binding of BzP to BSA are primarily non-ionic in nature. The number of binding sites (n) obtained are close to the reported values [16] indicating that there was only one independent class of binding site for BzP on BSA. The value of correlation coefficients obtained are closer to 0.9985, demonstrating that the BzP-BSA interactions agree well with the site binding model given by the equation (3).

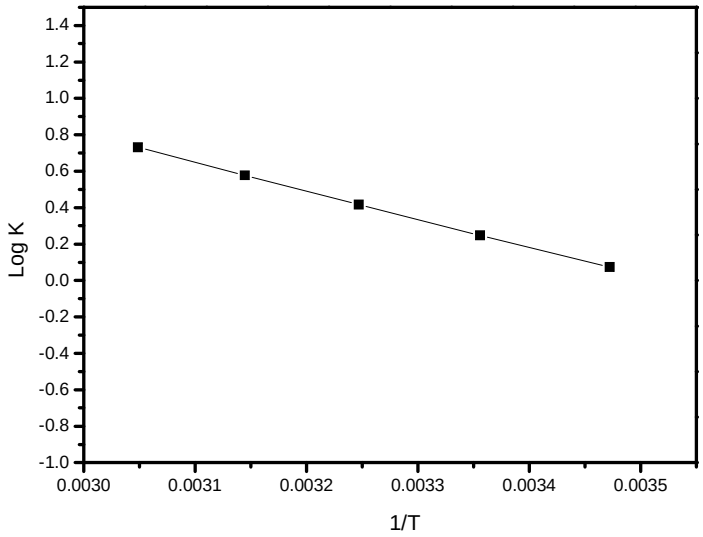

Fig. 5. The temperature dependent Stern-Volmer curves showing quenching of BSA with BzP

Table 1 Parameters of BzP-BSA interactions at various temperatures

Temp (K)	Binding constant $K \times 10^{-5}$ L mol^{-1}	R^2	No.of binding sites, *n*	ΔH^0 (k J mol^{-1})	ΔS^0 (J K^{-1} mol^{-1})	ΔG^0 (k J mol^{-1})
288	1.21	0.9939	0.88	29.69	103.85	-4.46
298	1.90	0.9889	0.98			
308	2.33	0.9882	1.09			
318	3.37	0.9864	1.32			
328	6.14	0.9862	1.89			

3.3. Thermodynamic parameters and the nature of binding forces

The thermodynamic parameters dependent on temperature were analyzed to differentiate the performing forces between BzP and BSA. The thermodynamic parameters involving the binding of BzP and BSA due to various acting forces like hydrogen bond, vanderwaals force, electro static force, hydrophobic interactions were found using van't hoffs equation.

$$\text{Log K} = -\Delta H^0/2.303\ RT + \Delta S^0/2.303R$$

The log *K* versus 1/T plot (Fig. 5) enabled the determination of ΔH^0 and ΔS^0 for the binding process. The value of ΔG^0 was calculated from the relation.

$$\Delta G^0 = \Delta H^0 - T\Delta S^0$$

Where ΔH^0, ΔG^0 and ΔS^0 are enthalpy change, free energy change, and entropy change respectively. The binding studies were carried out at 288, 298, 308, 318 and 328 K and the values of ΔH^0, ΔS^0 and ΔG^0 are listed in table 1. The negative sign of ΔG^0 values supported the assertion that all binding processes are spontaneous and that a folded state of BSA is favoured. From the table 1 it can be seen that ΔH^0 and ΔS^0 have positive values indicating that the binding is mainly entropy-driven and the enthalpy is unfavorable for it indicating that hydrophobic forces played a major role in the interaction leading to a folded state of BSA.

3.4. Absorption spectroscopic studies

UV-visible absorption spectroscopy was an effortless method, to determine the hydrophobic changes [17] and to know the configuration of the drug-protein complex.

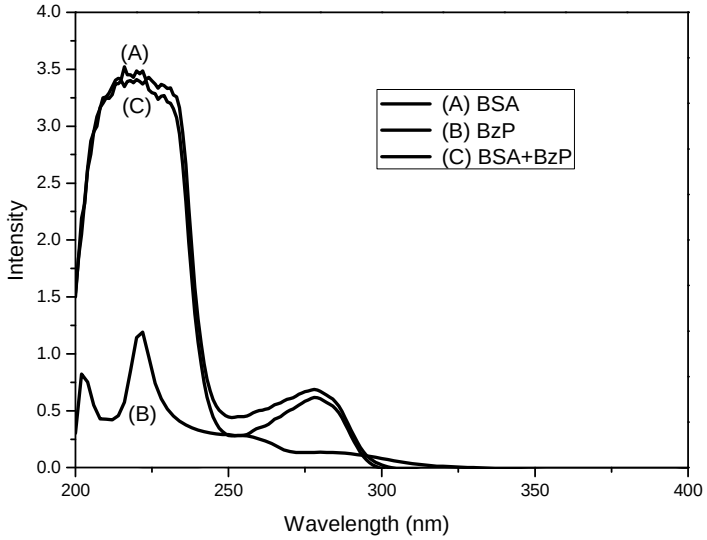

Fig. 6a. UV-vis absorption spectra of (a) BSA + BzP and (b) BzP

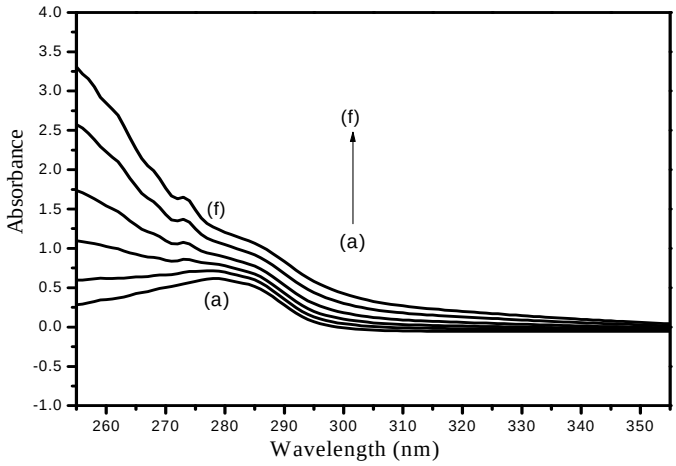

Fig. 6b. Absorption spectra of BSA (a) and BzP-BSA complex (b-f), BSA: 12 µM; BzP: 20 - 100 µM (b-f)

The λ_{max} of BSA at 286 nm was primarily due to the incidence of tryptophan and tyrosine residues in BSA. In the present study, we have recorded the absorption spectra of BzP and BSA, BzP-BSA complex (Fig. 6a), and noticed that the utmost peak position of BzP-BSA was to some extent shifted towards the lower wavelength region probably due to the complex configuration between BzP-BSA. From the absorption spectrum shown in Fig. 6b, it is clear that the intensity of absorption of BSA increased regularly with increasing concentration of BzP. The shift in the λ_{max} from 278 to 286 nm also proved the formation of a ground state complex in the interaction study.

3.5. Circular Dichroism studies

Further confirmation of changes in the secondary structure is obtained by recording Circular Dichroism (CD) spectra of BSA with and without the presence of BzP as shown in Fig. 7. It is clear from the bands obtained at 208 and 222 nm for BSA that its structure is primarily α-helical [18-21]. The initial decrease in the ellipticity with increasing wavelength is due to the negative cotton effect of the α-helical structure. The bands at 208 nm (-) arise from the excitonic splitting of the π-π* transition of the amidic groups, while the band at 222 nm (-) were due the n→π* transition.

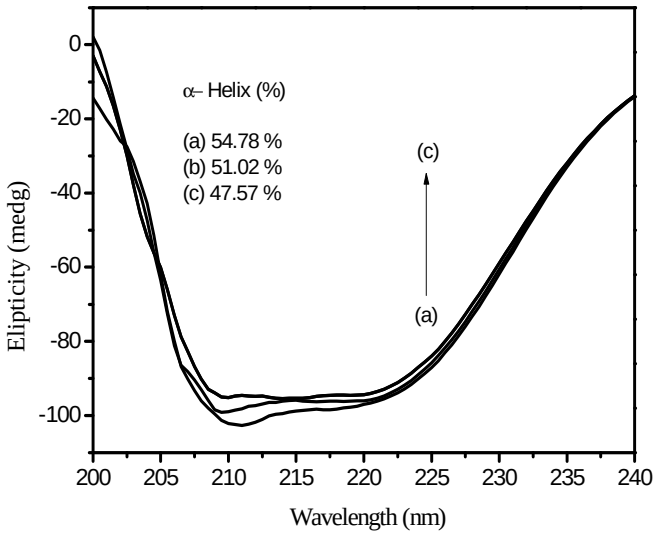

Fig. 7. CD spectra of BSA–BzP system: a) BSA; b) BSA + BzP (20 μM) and c) BSA + BzP (40 μM)

With increase in BzP concentration there is minor decrease in ellitpicity without any noticeable shift of the peaks, indicating that with the addition of BzP the secondary α-helical structure of BSA has changed. Furthermore, the reduction in negative ellipticity indicates an extended peptide strand, while the hydrophobicity was decreased leading to the folded state. The CD results were expressed [22] in terms of the mean residue ellipticity (MRE) in deg cm^2 $demo^{-1}$ according to Eq. 4.

$$\text{MRE} = \frac{\text{Observed CD (m deg)}}{\text{C}_\text{p}\ \text{nl x 10}} \qquad (4)$$

Where C_p is the molar concentration of protein, n is the number of amino acid residues and *l* is the path length. The α-helical contents of free and combined BSA were calculated from MRE values [23] at 208 nm using the Eq. 5.

$$\alpha - helix\ (\%) = \frac{\text{MRE}_{208} - 400}{33{,}000 - 4000} \times 100 \qquad (5)$$

Where MRE_{208} was the observed MRE value at 208 nm, 4000 was the MRE of the β-form and random coil conformations cross at 208 nm and 33,000 was the MRE value of a pair α-helix at 208 nm. From the Eqs. (4) and (5), the α-helicity in the secondary structure of BSA can be determined. The α-helicity in the secondary structure was calculated to be 54.78% in free BSA, and 47.57% on the BzP–BSA complex, indicating the loss of α-helicity upon interaction. The decrease in the α-helix structure indicated that the BzP was bound to the amino acid residues of the main polypeptide chain of BSA shattering their network of hydrogen bonds [24].

3.6. FT-IR spectroscopic studies

To get an insight on the changes in the amide group bands, FT-IR spectra of BSA was recorded with and without BzP as shown in Fig. 8. It is clear from the FT-IR spectrum of BSA protein that a number of amide bands appeared due to the different vibrational modes of the peptide moiety. The amides I (mainly C=O stretch) and II (C-N stretch coupled with N-H bending) peaks occurring in the region of 1600–1700 cm^{-1} and 1500–1600 cm^{-1}, respectively are the most widely used modes in the protein's secondary structural studies.

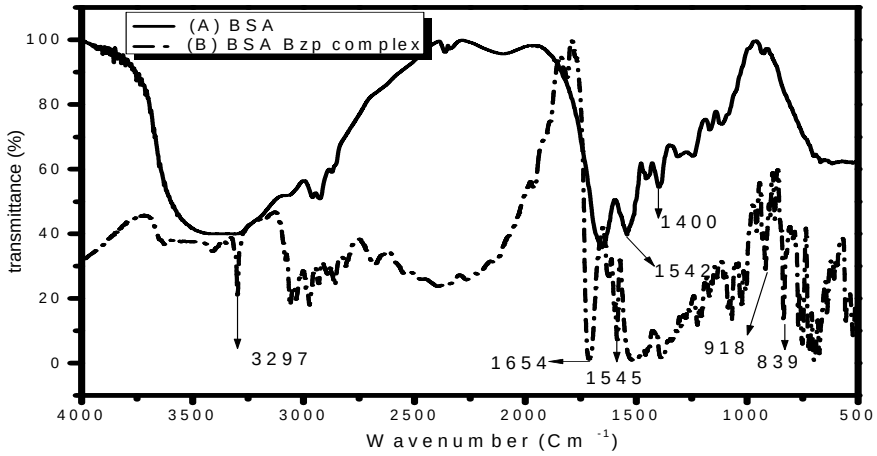

Fig. 8. Infrared spectra of (A) BSA (B) BSA-BzP complex

It is known that amide I band is more sensitive to changes in the protein secondary structure than the amide II band and hence used for studies of the BSA secondary structure [25-29]. To discover the changes of the BSA secondary structure, the FT-IR spectrum of BSA was recorded in the absence and presence of BzP. Fig. 8 shows the FT-IR spectra of free BSA and the dissimilarity spectra after binding with BzP. As seen from Fig. 8, the peak position of amide I band shifted from 1654 to 1600 cm^{-1} while that of the amide II band shifted from 1545 to 1516 cm^{-1}. This indicated that the secondary structure of the protein was changed due to the interaction between BzP and BSA.

3.7. Synchronous fluorescence spectra

Synchronous fluorescence was recorded for BSA with and without BzP, for evaluating the conformational changes of BSA as shown in Fig. 9. The environment of amino acid residues can be deliberated by measuring the emission wavelength (λ_{max}) shift, which is due to the change in the polarity around the chromophore molecule. When the $\Delta\lambda$ between the excitation wavelength and the emission wavelength was fixed at 15 nm or 60 nm, the synchronous fluorescence spectra of BSA can involve a change in the polarity of the micro-environment around tyrosine or tryptophan residues, respectively [30]. The maximum emission wavelength of Tyr residues remained principally unchanged, indicating that no discernable change occurred in the micro environment around Tyr residues during the binding process.

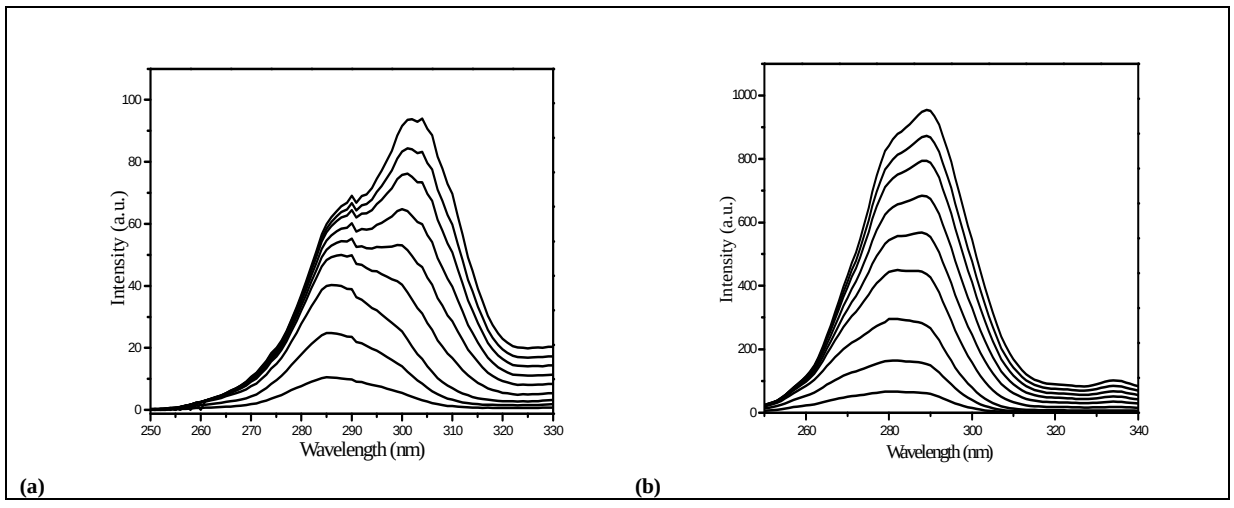

Fig. 9. Synchronous fluorescence spectra of BSA– BzP: (A) For $\Delta\lambda$=15 nm while for (B) $\Delta\lambda$=60 nm, the concentration of BSA was 12 µM, the concentration of BzP: (a) 20-200 µM

On the other hand, the maximum emission wavelength of Trp residues has a slight blue-shift, indicating that the polarity around Trp residues micro-regions decreased and the hydrophobicity increased upon interaction with BzP. Also the field of quenching at $\Delta\lambda$ = 60 nm was higher than that of $\Delta\lambda$ = 15 nm, implying that BzP was more rapidly

bound to Trp residues compared to Tyr residues. Hence it is proven that the binding sites are mainly focused on tryptophan moiety [31] that is responsible for the conformational changes in the secondary structure of BSA.

CONCLUSION

The present work focuses on the interaction of BzP with BSA with the help of different spectroscopic techniques. The results showed that the BSA fluorescence was quenched by BzP through the static quenching mechanism. The UV, CD, synchronous flouroscence and FT-IR spectral studies confirmed that binding of BzP with BSA induces a change in the secondary structure of the protein. It was also found that there is only one binding site for BzP to BSA. The negative Gibb's free energy change indicated that the process of binding was spontaneous. The absorption spectra and CD spectra showed that the conformation of BSA has been changed in the presence of BzP. All these results reveal that BzP binds to BSA effectively which would be useful in the pharmaceutical industry, life sciences and clinical medicine.

Acknowledgement
The authors are grateful to VIT University, Vellore for recording all the spectral data and MC is greatful for the financial support from VIT Chennai campus. The authors declare no conflict of interest regarding the publication of this paper.

REFERENCES

[1] Kragh-Hansen U, *Pharmacol Rev.*, **1981**, 33, 53.
[2] Zhang HX, Huang X, Mei P et al., *J Fluorescence.*, **2006**, 16, 287.
[3] Sulkowska A, *J. Mol Struct* **2002** 614, 232.
[4] Guharay J, Sengupta B, Sengupta PK , *fluorescence spectroscopic study Proteins.*, **2001**, 43, 81.
[5] Liu JQ, Tian JN, Zhang JY et al., *Anal Bioanal Chem.*, 2003, 376, 867.
[6] Wang YQ, Zhang HM, Zhang GC et al., *J. Pharm Biomed Anal.*, **2007**, 43, 1875.
[7] Gelamo EL, Tabak M, *Spectrochim Acta Pt A-Mol Bio.*, **2000**, 56, 2271.
[8] Maurice RE, Camillo AG, *Anal Biochem.*, **1981**, 114 212.
[9] Ware WR, *J. Phys Chem.*, **1962**, 66, 458.
[10] Tian JN, Liu JQ, Zhang JY et al., *Chem Pharm Bul.*, **2003**, l51, 582.
[11] Lakowicz JR, Principle of fluorescence spectroscopy, 3rd edn. Springer, New York, **1999**
[12] Bi S, Song D, Tian Y et al., *Spectrochim Acta Pt A-Mol Bio.*, **2005**, 61, 636.
[13] Tian JN, Liu JQ, Hu ZD, Chen XG, *Bioorg Med Chem.*, **2005**, 13, 4129.
[14] Li Y, He W, Liu J et al., *Biochim Biophys Acta.*, **2005,** 17, 21
[15] Nithya.P, Nawaz khan.F, Mohan roopan. S, et.al., *chemical papers*., **2011**, 65(5), 743.
[16] Jiang M, Xie MX, Zheng D et al., *J. Mol Struct.*, **2004**, 692, 80.
[17] Yang P, Gao F, The principle of bioinorganic chemistry. Science Press, p 349, **2002**.
[18] Lehrer SS, *Biochemistry*., **1971**, 10, 3263.
[19] Keerti M. Naik, Sharanappa T. Nandibewoor, *J. Lumin.*, **2013**, 143, 491.
[20] Zhang Y, Zhou B, Liu Y, et.al., *J . Fluoresc*., **2008**, 18, 118.
[21] Kandagal PB, Ashoka S, Seetharamappa J, et.al., *J . Pharm Biomed.*, **2006**, 41, 399.
[22] Wang YQ, Zhang HM, Zhang GC, et.al., *Int J. Biol Macromol.*, **2007**, 41, 250
[23] Sun SF, Zhou B, Hou HN, et.al., *Int J. Biol Macromol.*, **2006**, 39, 200.
[24] Hu YJ, Liu Y, Wang JB, et.al., *J. Pharm Biomed Anal.*, 36, **2004**, 919.
[25] Ross PD, Subramanian S, *Biochemistry.*, **1981**, 20, 3102.
[26] Lu ZX, Cui T, Shi QL, In molecular biology, applications of circular dichroism and optical rotatory dispersion, 1st ed. Science Press, pp79–82, **1987**.
[27] Ashoka S, Seetharamappa J, et.al., *J. Luminesc.*, **2006**, 121,186.
[28] Ashoka S, Seetharamappa J, et.al., *J. Molecular structure.*, **2006**, 786, 52.
[29] Kamat BP, Seetharamappa J, *J. Pharmaceutical & Biomed analysis.*, **2004**, 35, 664.
[30] Papadopoulou A, Green RJ, Frazier RA, *J. Agric Food Chem.*, **2005**, 53,163
[31] Cyril L, Earl JK, Sperry WM, In: Biochemists' handbook, E & FN Spon, London, pp 84, **1961**.